

Energetics of the Proton Transfer Pathway for Tyrosine D in Photosystem II

Keisuke Saito,^{A,B,C} Naoki Sakashita,^A and Hiroshi Ishikita^{A,B}

^ADepartment of Applied Chemistry, The University of Tokyo, 7-3-1 Hongo, Bunkyo-ku, Tokyo 113-8654, Japan.

^BResearch Center for Advanced Science and Technology, The University of Tokyo, 4-6-1 Komaba, Meguro-ku, Tokyo 153-8904, Japan.

^CCorresponding author. Email: ksaito@appchem.t.u-tokyo.ac.jp

The proton transfer pathway for redox active tyrosine D (TyrD) in photosystem II is a hydrogen-bond network that involves D2-Arg180 and a series of water molecules. Using quantum mechanical/molecular mechanical calculations, the detailed properties of the energetics and structural geometries were investigated. The potential-energy profile of all hydrogen bonds along the proton transfer pathway indicates that the overall proton transfer from TyrD is energetically downhill. D2-Arg180 plays a key role in the proton transfer pathway, providing a driving force for proton transfer, maintaining the hydrogen-bond network structure, stabilising P680^{•+}, and thus deprotonating TyrD-OH to TyrD-O[•]. A hydrophobic environment near TyrD enhances the electrostatic interactions between TyrD and redox active groups, e.g. P680 and the catalytic Mn₄CaO₅ cluster: the redox states of those groups are linked with the protonation state of TyrD, i.e. release of the proton from TyrD. Thus, the proton transfer pathway from TyrD may ultimately contribute to the conversion of S₀ into S₁ in the dark in order to stabilise the Mn₄CaO₅ cluster when the photocycle is interrupted in S₀.

Manuscript received: 19 April 2016.

Manuscript accepted: 29 May 2016.

Published online: 4 July 2016.

Introduction

In photosystem II (PSII), the chlorophyll dimer P680 is composed of four chlorophyll *a* molecules, P_{D1}, P_{D2}, Chl_{D1}, and Chl_{D2}, and it absorbs light at a wavelength of 680 nm, leading to the formation of a range of charge-separated states with P680^{•+}. These states are stabilized by electron transfer to the first quinone, Q_A, and by electron donation from a tyrosine residue, tyrosine Z (TyrZ, D1-Tyr161), to P680^{•+} (\approx P_{D1}^{•+}). TyrZ then oxidizes the water-oxidizing Mn₄CaO₅ cluster. Oxidation of the Mn₄CaO₅ cluster occurs in the S₀ → S₁ → S₂ → S₃ → S₀ transitions (as previously reviewed^[1]). To serve as a redox active cofactor, TyrZ requires the hydrogen-bond partner D1-His190. Recently determined high-resolution PSII crystal structures^[2] revealed that the phenolic O site of TyrZ forms a hydrogen bond with the N ϵ site of D1-His190 with an O_{TyrZ}–N ϵ _{D1-His190} length of \sim 2.5 Å. The significantly shortened hydrogen-bond distance was not one of the most significant points about the crystal structure^[2a] until Saito et al. demonstrated that the remarkably short hydrogen-bond distance can be quantum-chemically reproduced in the presence of the PSII protein environment.^[3] The pK_a values of TyrZ and D1-His190 are equal in the PSII protein environment,^[3] leading to the formation of a significantly short, ‘single-well hydrogen bond’.^[4] The proton is localized near the hydrogen-bond donor moiety in standard hydrogen bonds. In contrast, the proton is delocalized at the bottom of the nearly barrierless potential in single-well hydrogen bonds, which appears to be a theoretical basis for the so-called ‘proton-rocking mechanism’ of TyrZ

(e.g.^[3,5]), where the proton that belongs to the N ϵ site of D1-His190 is deprotonatable (note: this is energetically possible because the N δ site donates a hydrogen bond to D1-Asn298 and is permanently protonated). Thus, the proton-rocking mechanism is possible only when the proton in the hydrogen bond can belong to both TyrZ and D1-His190 either (i) by having TyrZ and D1-His190 with similar pK_a values in a single-well hydrogen bond, or (ii) by having the two cases, pK_a(TyrZ) \geq pK_a(D1-His190) and pK_a(TyrZ) \leq pK_a(D1-His190), depending on the TyrZ redox state: this means that the *proton-rocking model requires the deprotonatable H⁺ at the N ϵ site of D1-His190* (Fig. 1a).

In PSII, another redox active tyrosine, tyrosine D (TyrD, D2-Tyr160), has D2-His189 as a hydrogen-bond partner. Because TyrD is geometrically isolated from the electron transfer pathway from the Mn₄CaO₅ cluster to P680 via TyrZ, it plays no obligatory role in enzyme function. It was generally thought that the phenolic proton of TyrD was most likely to transfer to the N ϵ site of D2-His189 (e.g.^[6]), as is the case for the TyrZ–D2-His190 pair (summarized by Nakamura and Noguchi^[7]). However, this appears to be impossible based on the geometry of the crystal structures. Ishikita and Knapp found that in contrast to D1-His190, the putative proton-rocking N ϵ site of D2-His189 cannot release the proton (unless D2-His189 becomes the doubly deprotonated anionic form), because the *N ϵ site of D2-His189 is permanently protonated owing to the N δ site of D2-His189 being hydrogen bonded by positively charged D2-Arg294* (Fig. 1b).^[8]

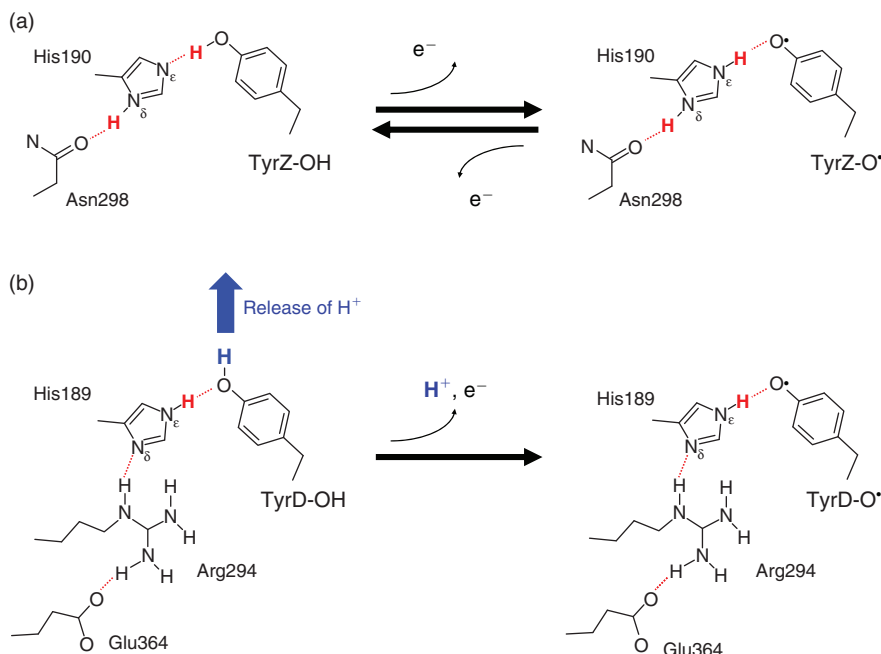


Fig. 1. The releasing (blue) and remaining (red) protons near TyrZ and TyrD. (a) TyrZ. N δ of D1-His190 is permanently protonated due to the presence of the carbonyl O of D1-Asn298.^[8] Thus, a hydrogen atom is always present between N ϵ of D1-His190 and the phenolic O of TyrZ, irrespective of the TyrZ redox state. (b) TyrD. N δ of D2-His189 is permanently deprotonated due to the presence of D2-Arg294.^[8] Thus, TyrD-OH can never donate a hydrogen bond to N ϵ of D2-His189 (i.e. the hydrogen atom between D2-His189 and TyrD always belongs to N ϵ of D2-His189). Therefore, TyrD-OH must release the phenolic proton towards the protein surface via the proton transfer pathway once it is oxidized to TyrD-O \bullet .^[9]

In contrast, the permanently protonated N ϵ site of D2-His189 forces the -OH group of TyrD-OH to orient out of the TyrD–D2-His189 bond towards an external water molecule H $_2$ O $_D$ (Fig. 2) when TyrD-OH is formed.^[9] H $_2$ O $_D$ has two binding positions, H $_2$ O $_D$ (prox) and H $_2$ O $_D$ (dist),^[2] and it moves between TyrD and D2-Arg180 in response to changes in the TyrD oxidation state.^[9] Using large-scale quantum mechanical/molecular mechanical (QM/MM) calculations and the crystal structure,^[2a] Saito et al. demonstrated that in response to oxidation of TyrD-OH to TyrD-O \bullet , the proton released from TyrD-OH is transferred along the proton transfer pathway involving D2-Arg180, D2-His61, and a series of water molecules (i.e. redox-coupled proton transfer).^[9] Intriguingly, the corresponding pathway is also conserved on the active D1 side, involving TyrZ, water molecules adjacent to the Mn $_4$ CaO $_5$ cluster, a Cl $^-$ ion interacting with D1-Asn181, and D1-Asp61;^[9] this implies that in an ancestral homodimer, there was once an active Mn cluster in the cavity adjacent to TyrD.^[10]

Notably, the proton transfer pathway from TyrD suggested by Saito et al. has been supported by recent FT-IR spectroscopy studies by Nakamura and Noguchi, where the release of the proton to the bulk was observed in response to the oxidation of TyrD-OH.^[7] In the present study, we determined the detailed properties of energetics and structural geometries of the proton transfer pathway from TyrD.

Results and Discussion

Geometry and Energy Profile Along the Proton Transfer Pathway

The proton transfer pathway from TyrD^[9] is consistent with a hydrogen-bond network that has six water molecules conserved

in the 1.9 Å^[2a] and the free electron laser structures.^[2b] The hydrogen-bond network is located along the cavity with a length of \sim 24 Å (Fig. 2a). H $_2$ O $_D$, the initial proton acceptor from TyrD, is spatially isolated from the other five water molecules by the D2-Arg180 side chain (Fig. 2b).

Fig. 3a shows the potential-energy profile of all hydrogen bonds along the proton transfer pathway. The potential-energy profile indicates that overall proton transfer from TyrD is energetically downhill (Fig. 3a). The energy levels at the proton acceptor moieties along the pathway are consistent with those reported previously.^[9] As proton transfer proceeds, the hydrogen-bond pattern of the entire proton transfer pathway is altered from the ‘pre-PT’ pattern to the ‘post-PT’ pattern (Fig. 4a). The downhill proton transfer steps from W480 to W373 (Fig. 4b) and from W373 to W783 (Fig. 4c) involve rearrangement of the hydrogen-bond network. The radical state was fully localized on TyrD-O \bullet in the QM region (Fig. 3b).

Remarkably, the region near the TyrD (D2-Tyr160)/D2-His189 pair is hydrophobic because of the localization of several hydrophobic phenylalanine side chains near the TyrD/D2-His189 pair, e.g. D2-Phe181, D2-Phe184, D2-Phe185, and CP47-Phe362^[8] (Figs 2c and 5), which destabilize the proton released from TyrD and serve as a driving force for proton transfer once TyrD-OH is oxidized. The proton transfer from D2-Arg180 to W373 is significantly downhill (Fig. 3a) because the acceptor W373 forms a hydrogen bond with negatively charged D2-Asp333 and provides a driving force for the proton transfer from the positively charged donor D2-Arg180 (Fig. 5).

Roles of D2-Arg180 in Proton Transfer from TyrD

It appears that D2-Arg180 is a key component that plays a role in releasing a proton from TyrD-OH and forming TyrD-O \bullet ,

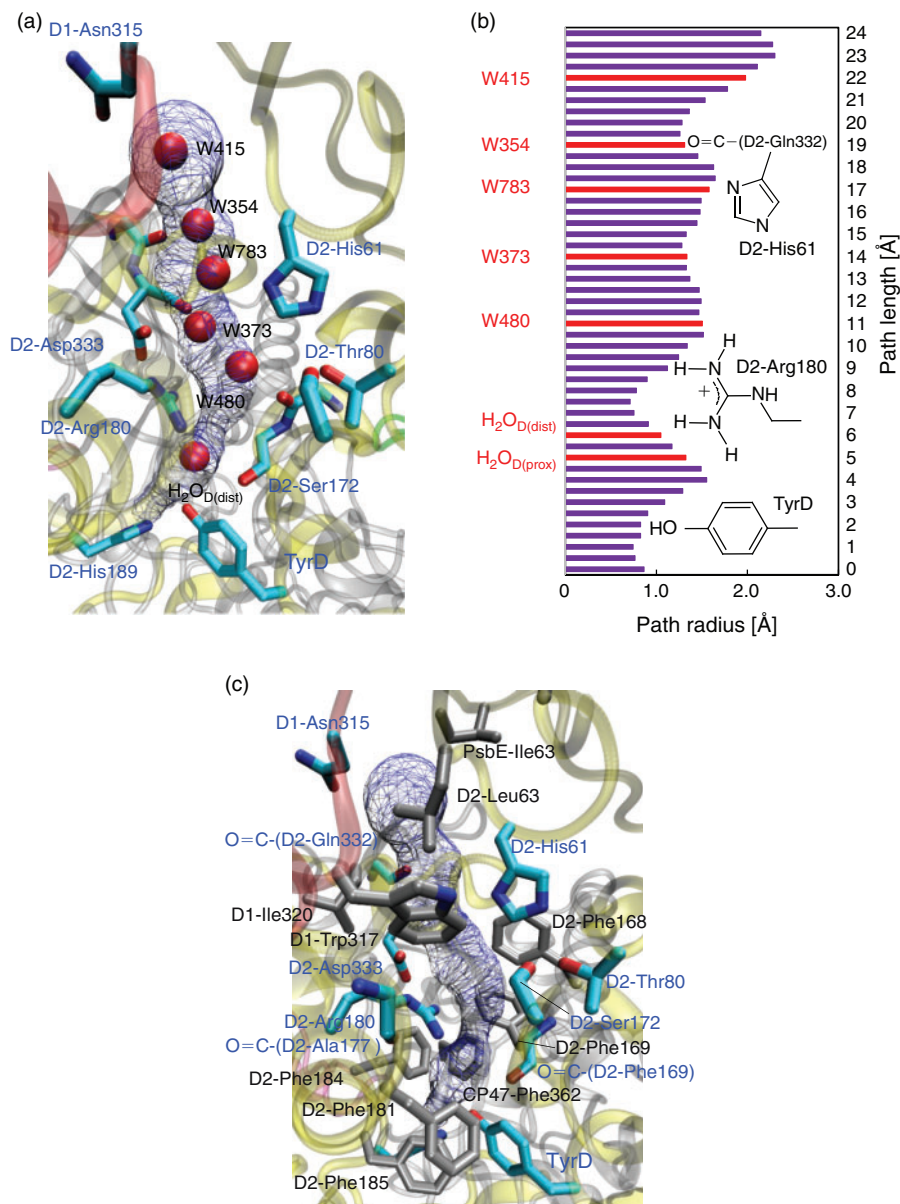


Fig. 2. Water molecules along the proton transfer pathway for TyrD. (a) Location of water molecules identified in the 1.9 Å structure^[2a] (depicted as red balls) along the cavity (blue mesh). The channel space was analyzed using the program CAVER.^[23] (b) The cavity radii (path radii) along the proton transfer pathway in Angstrom. Red lines indicate path radii near the water molecules. (c) Localization of hydrophobic (black labels) and polar (blue labels) groups near TyrD.

because (i) D2-Arg180 is the only titratable side chain involved in the proton conducting hydrogen-bond network via TyrD (Fig. 2) and (ii) in the D2-Arg180 mutants, the electron paramagnetic resonance (EPR) signals from TyrD (i.e. TyrD-O[•]) were small.^[11] Considering the energy profile of the TyrD proton transfer presented here, the following roles of D2-Arg180 can be postulated:

D2-Arg180, Providing a Driving Force for the Proton Transfer

As described above, mutation of positively charged D2-Arg180 (i.e. loss of the positive charge) should result in a decrease in the driving force for the downhill proton transfer, specifically from D2-Arg180 to W373 (Fig. 3a), and loss of the TyrD-O[•] formation; this may explain why the D2-Arg180

mutation resulted in the decrease of the EPR signal from TyrD.^[11]

D2-Arg180, Maintaining the Hydrogen-Bond Network Structure

D2-Arg180 is the only titratable side chain involved in the proton-conducting hydrogen-bond network from TyrD (Fig. 2). The removal of D2-Arg180 may result in the disorder of the hydrogen-bond network, leading to an increase in the activation energy for proton transfer (e.g.^[12]).

D2-Arg180, Stabilizing P680^{•+} and Deprotonating TyrD-OH

D2-Arg180 also contributes to increasing the P_{D1}^{•+} population.^[13] Indeed, mutations at the D2-Arg180 residue have been

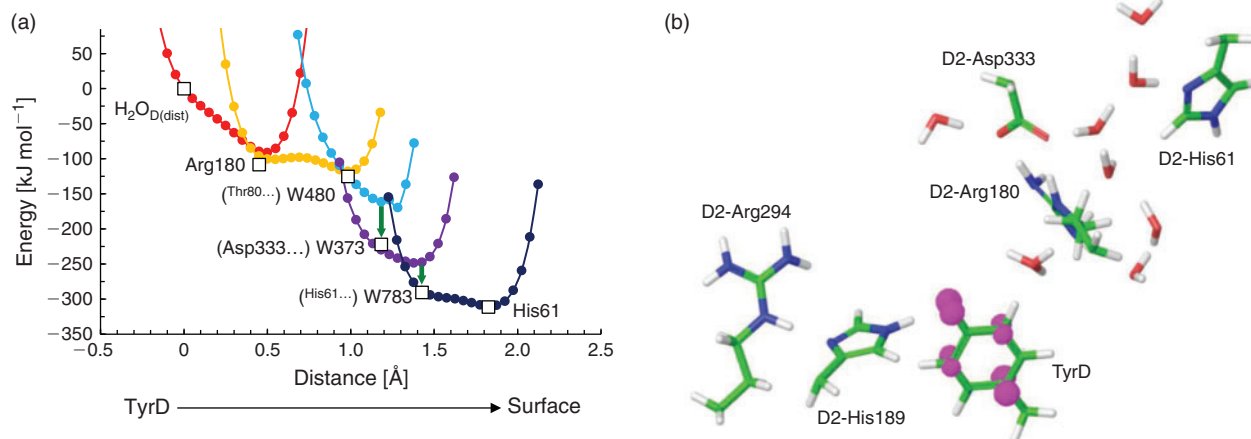


Fig. 3. The proton transfer pathway from TyrD. (a) Potential-energy profile of all hydrogen bonds along the proton transfer pathway. Open squares indicate the energy levels along the proton transfer pathway reported by Saito et al.^[91] which are consistent with the potential-energy profile presented here. Vertical lines (green) indicate rearrangement processes of the hydrogen-bond network shown in Fig. 4b, c. (b) The spin density distribution (magenta sphere) in the QM region.

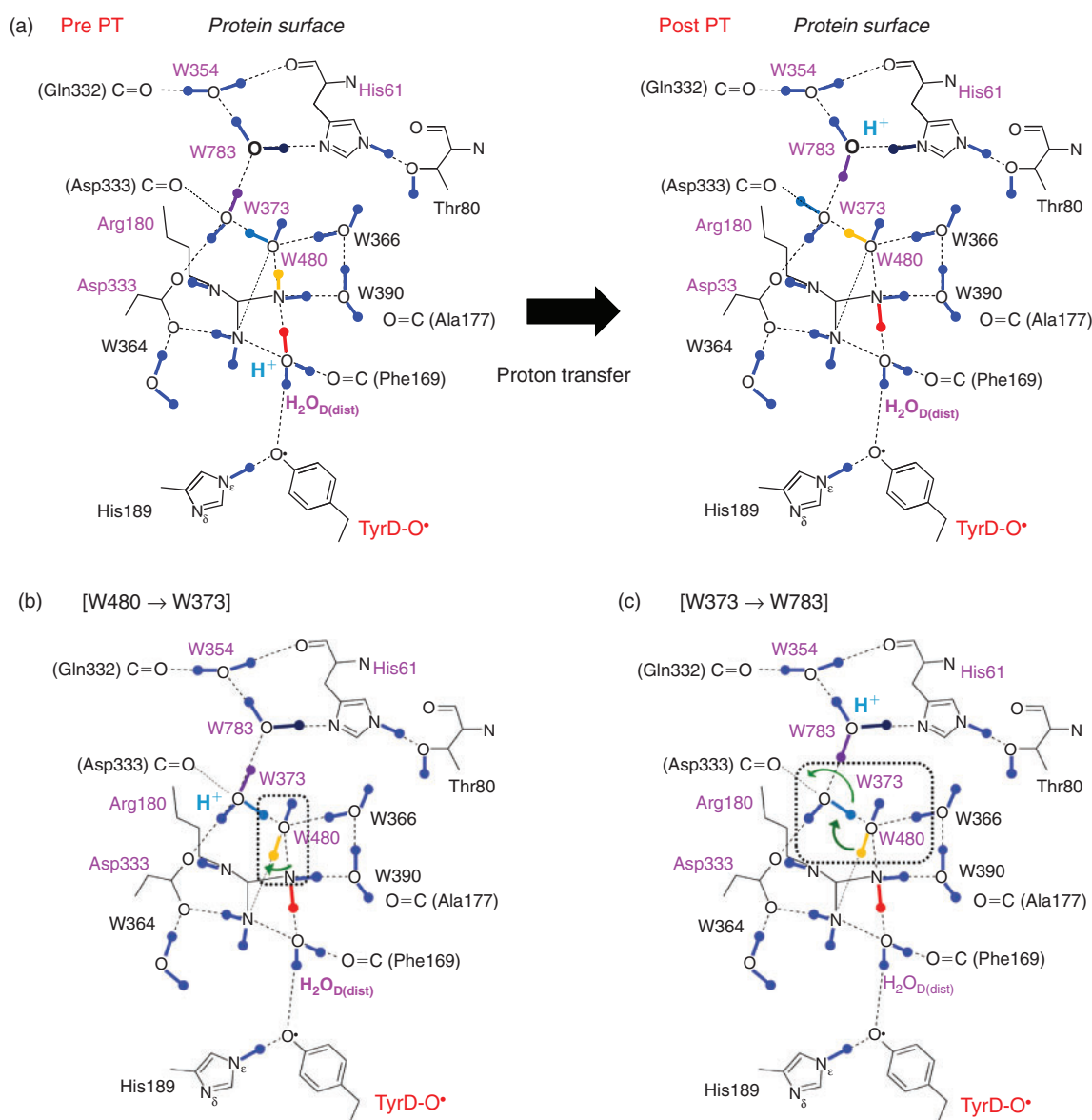


Fig. 4. Hydrogen-bond patterns of the proton transfer pathway from TyrD observed (a) before (pre-PT) and after proton transfer (post-PT), and observed rearrangement of the hydrogen-bond network associated with proton transfers (b) from W480 to W373 and (c) from W373 to W783. Arrows (green) indicate reorientation of H-bonds.

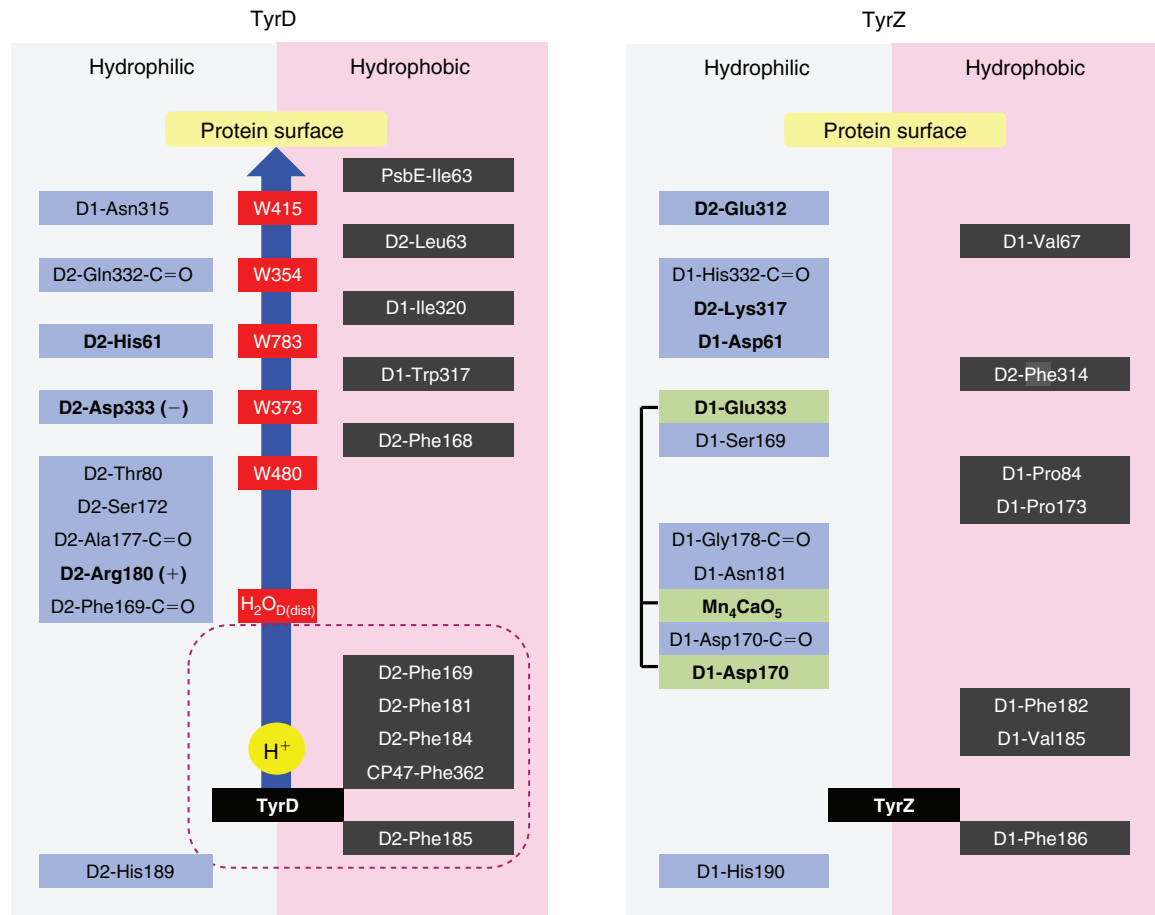


Fig. 5. List of hydrophobic (gray) and hydrophilic (blue) residues along the proton transfer pathway from TyrD (left). The corresponding residues on the TyrZ side are also listed (right).

shown to increase the charge recombination rate between $Q_A^{\bullet-}$ and $P680^{\bullet+}$ ($\approx P_{D1}^{\bullet+}$), i.e. destabilize $P680^{\bullet+}$.^[11] Rutherford et al. proposed that TyrD-O \bullet formation was associated with localization of the highly oxidizing cation $P680^{\bullet+}$ to the chlorophyll nearest to TyrZ (i.e. $P_{D1}^{\bullet+}$) for efficient electron transfer from the Mn_4CaO_5 cluster via TyrZ;^[14c] this may be understood by considering the presence of D2-Arg180, which has an electrostatic link with both TyrD and $P680^{\bullet+}$. These observations may represent a functional link between the ‘formation of $P_{D1}^{\bullet+}$ ’ and ‘release of the proton from TyrD-OH (i.e. formation of TyrD-O \bullet)’ mediated by D2-Arg180.

When TyrD Uses the Proton Transfer Pathway: Electron Transfer via TyrD

A hydrophobic environment of TyrD in comparison with TyrZ (e.g.^[2a,8,9,14c,15]) makes TyrD sensitive to the redox states of the other redox-active cofactors, e.g. P680 and the Mn_4CaO_5 cluster (e.g.^[14c]). TyrD is involved in the following electron transfer processes (e.g.^[14c]):

Electron Transfer from TyrD-OH to $P680^{\bullet+}$ (Fig. 6a)

The release of the proton from TyrD-OH was observed even in the Mn_4CaO_5 -depleted PSII in response to the formation of $P680^{\bullet+}$ (e.g.^[7,14]). TyrD-OH transfers the electron to highly oxidizing $P680^{\bullet+}$ and simultaneously releases the proton. This occurs on a time scale in the tens of milliseconds.^[14b,16]

Electron Transfer from TyrD-OH to S_2 (Fig. 6b)

EPR studies demonstrated that S_2 can be reduced to S_1 by TyrD-OH in the dark (1–2 s);^[14c,17] this is possible because TyrD-O \bullet /TyrD-O has a redox potential of ~ 0.7 V^[8,18], which is lower than ~ 0.9 V for S_1/S_2 .^[18]

Electron Transfer from S_0 to TyrD-O \bullet (Fig. 6c)

Once formed, TyrD-O \bullet is very stable for many hours.^[14a,14c] Long dark adaptation of PSII resulted in the oxidation of S_0 to S_1 via electron transfer from S_0 ($S_0/S_1 \sim 0.7$ V^[18]) to TyrD-O \bullet .^[14c,17] In pea thylakoids, S_0 disappears in ~ 20 min.^[17a] In addition, TyrD oxidizes the over-reduced states of the Mn_4CaO_5 cluster, e.g. S_{-1} and S_{-2} (‘photoactivation’^[19]).

Among the three cases, electron transfer from TyrD-OH to $P680^{\bullet+}$ ^[7,14] (Fig. 6a) or electron transfer from TyrD-OH to S_2 ^[14c,17] (Fig. 6b) requires the release of the proton from TyrD-OH along the proton transfer pathway, resulting in TyrD-O \bullet . TyrD-O \bullet is stable for many hours and can oxidize S_0 to S_1 in the dark, resulting in a 100% S_1 sample.^[14a,14c] Since TyrD-O \bullet is frequently present in PSII samples,^[14a,14c] it is possible that the proton transfer pathway from TyrD^[9] functions to facilitate the formation of TyrD-O \bullet , which is ready for a conversion of S_0 into S_1 in the dark,^[14c,17] presumably to stabilize the Mn_4CaO_5 cluster (e.g.^[19]). All these redox roles of TyrD^[14c] are possible because of the hydrophobic environment of TyrD,^[2a,8,9,14c,15] where electrostatic interactions are pronounced.

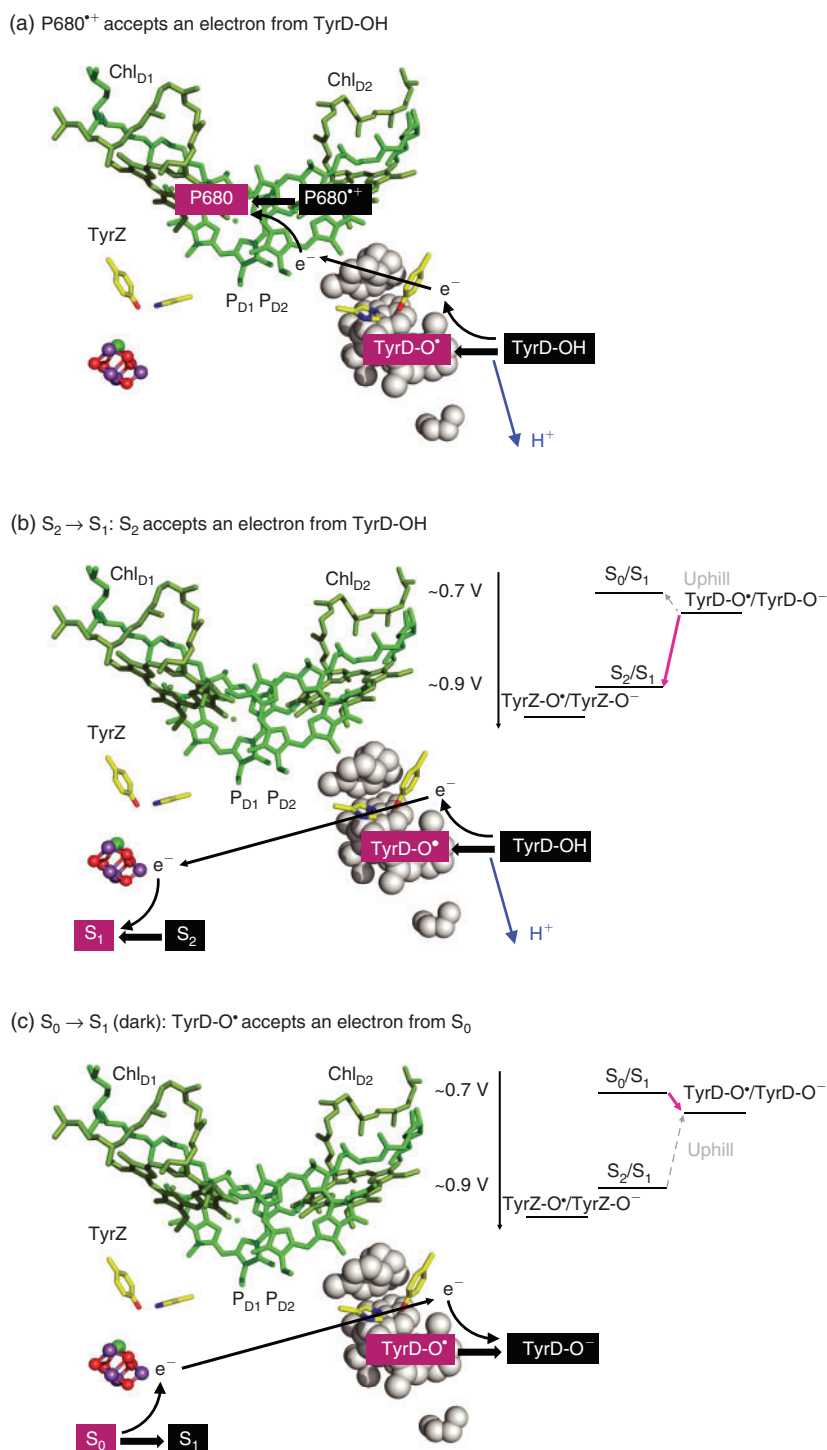


Fig. 6. Electron transfer mediated by TyrD (black arrows) and proton transfer from TyrD-OH (blue arrows). (a) Electron transfer from TyrD-OH to $P680^{*+}$. (b) Electron transfer from TyrD-OH to the Mn_4CaO_5 cluster in S_2 . (c) Electron transfer from the Mn_4CaO_5 cluster in S_0 to TyrD-O* ('dark adaptation'^[14c,17]).

Concluding Remarks

The proton transfer pathway that proceeds from TyrD towards the protein bulk surface, originally suggested in QM/MM studies^[9] and further confirmed in recent FT-IR spectroscopy studies,^[7] is present in all recent high-resolution crystal structures^[2] (Table 1). The potential-energy profile of all hydrogen bonds along the proton transfer pathway indicates that the

overall proton transfer from TyrD is energetically downhill (Fig. 3). D2-Arg180 plays a key role in the proton-conducting pathway, providing a driving force for proton transfer, maintaining the hydrogen-bond network structure as being the only titratable residue in the pathway (Figs. 2 and 4), stabilizing $P680^{*+}$ ^[11] (in particular by increasing the P_{D1}^{*+} population over the P_{D2}^{*+} population^[13]), and thus deprotonating TyrD-OH

Table 1. B-factor values of water molecules in the proton transfer pathway from TyrD^[9]

Water ^A	PDB ID (monomer unit)					
	3ARC (A)	3ARC (B)	4UB6 (A)	4UB6 (B)	4UB8 (A)	4UB8 (B)
H ₂ O _{D(prox)} (occupancy)	19.27 (0.35)	23.13 (0.40)	23.33 (0.65)	19.09 (0.40)	15.82 (0.35)	20.31 (0.40)
H ₂ O _{D(dist)} (occupancy)	20.14 (0.65)	24.68 (0.60)	14.15 (0.35)	19.52 (0.60)	20.56 (0.65)	20.75 (0.60)
390D	22.28	27.08	16.45	25.27	18.42	23.86
366D	19.03	19.82	16.31	24.44	17.15	23.00
480D	26.49	32.62	23.82	22.98	33.12	29.21
373D	23.66	23.18	19.17	27.06	18.92	23.88
783D	41.15	45.18	30.16	22.52	32.48	41.53
354D	36.35	41.08	41.45	23.01	33.27	42.31
415D	44.73	45.56	39.41	31.12	40.26	42.28

^ARepresented by labels used in 3ARC (A).

to TyrD-O[•].^[7,14] Deprotonation of D2-Arg180 predominantly decreases the redox potential of TyrD but not that of TyrZ owing to the hydrophobic environment, which is formed by phenylalanine side chains near the TyrD/D2-His189 pair, e.g. D2-Phe181, D2-Phe184, D2-Phe185, and CP47-Phe362 as suggested previously.^[8] The hydrophobic environment near TyrD also enhances the electrostatic interaction of TyrD with redox active cofactors, e.g. P680^{•+} (Fig. 6a) and the Mn₄CaO₅ cluster (Fig. 6b, c). In particular, the conversion of S₀ into S₁ in the dark (dark adaptation) is a redox role of TyrD-O[•].^[14c,17b] It can be postulated that the proton transfer pathway from TyrD ultimately contributes to the conversion of S₀ into S₁ in the dark to stabilize the Mn₄CaO₅ cluster when the photocycle is interrupted in S₀.

Computational Procedures

The atomic coordinates of PSII were taken from the X-ray structure of the PSII monomer unit designated monomer A of the PSII complexes from *Thermosynechococcus vulcanus* at a 1.9 Å resolution (PDB code, 3ARC).^[2a] Owing to the large system size of PSII, we considered residues and cofactors in subunits D1, D2, CP47, and CP43 only as the protein environment.^[9] Hydrogen atoms were generated and energetically optimized using CHARMM,^[20] whereas the positions of all non-hydrogen atoms were fixed and all titratable groups were kept in their standard protonation states. For the QM/MM calculations, we added additional counter ions to neutralize the entire system. Atomic partial charges of the amino acids were adopted from the all-atom CHARMM22^[21] parameter set. The atomic charges of the cofactors were taken from our previous studies of PSII.^[9]

We used the *Qsite*^[22] program code as described in previous studies.^[9] We employed the unrestricted density functional theory method with the B3LYP functional and LACVP**+ basis sets. The geometries were refined by constrained QM/MM optimization (see Supplementary Material). Specifically, the coordinates of the heavy atoms in the surrounding MM region were fixed to the original X-ray coordinates, whereas those of the hydrogen atoms in the MM region of the residues within 7.0 Å from the QM region were optimized using the OPLS2005 force field. All atomic coordinates in the QM region were fully relaxed (i.e. not fixed) in the QM/MM calculation. The QM region was defined as: D2-His61, TyrD, D2-Arg180, D2-His189, D2-Arg294, D2-Asp333, and water molecules that were within hydrogen-bond distance of these residues, namely, HOH-(chain D)-1(H₂O_D), -D354, -D364,

-D366, -D373, -D390, -D480, and -D783. The potential-energy profile of the hydrogen bond was obtained as follows: first, we prepared for the QM/MM optimized geometry without constraints, and we used the resulting geometry as the initial geometry. The hydrogen atom was then moved from the hydrogen-bond donor atom (e.g. O_{donor}) to the acceptor atom (e.g. O_{acceptor}) by 0.05 Å, after which the geometry was optimized by constraining the O_{donor}-H and H-O_{acceptor} distances, and the energy of the resulting geometry was calculated. This procedure was repeated until the hydrogen atom reached the O_{acceptor} atom.

Supplementary Material

The QM/MM optimized geometries are available on the Journal's website.

Acknowledgements

This research was supported by the JST PRESTO program (K.S.), JSPS KAKENHI (22740276 and 26800224 to K.S. and 15H00864, 26105012 and 26711008 to H.I.), Materials Integration for Engineering Polymers of Cross-Ministerial Strategic Innovation Promotion Program (SIP, H.I.), Tokyo Ohka Foundation for The Promotion of Science and Technology (H.I.), and Interdisciplinary Computational Science Program in CCS, University of Tsukuba. Theoretical calculations were partly performed using the Research Center for Computational Science, Okazaki, Japan.

References

- [1] (a) H. Dau, I. Zaharieva, M. Haumann, *Curr. Opin. Chem. Biol.* **2012**, *16*, 3. doi:10.1016/J.CBPA.2012.02.011
(b) N. Cox, J. Messinger, *Biochim. Biophys. Acta* **2013**, *1827*, 1020. doi:10.1016/J.BBABI.2013.01.013
- [2] (a) Y. Umena, K. Kawakami, J.-R. Shen, N. Kamiya, *Nature* **2011**, *473*, 55. doi:10.1038/NATURE09913
(b) M. Suga, F. Akita, K. Hirata, G. Ueno, H. Murakami, Y. Nakajima, T. Shimizu, K. Yamashita, M. Yamamoto, H. Ago, J.-R. Shen, *Nature* **2015**, *517*, 99. doi:10.1038/NATURE13991
- [3] K. Saito, J.-R. Shen, T. Ishida, H. Ishikita, *Biochemistry* **2011**, *50*, 9836. doi:10.1021/BI201366J
- [4] (a) A. Warshel, A. Papazyan, P. A. Kollman, *Science* **1995**, *269*, 102. doi:10.1126/SCIENCE.7661987
(b) C. L. Perrin, J. B. Nielson, *Annu. Rev. Phys. Chem.* **1997**, *48*, 511. doi:10.1146/ANNUREV.PHYSICHEM.48.1.511
- [5] (a) R. Ahlbrink, M. Haumann, D. Cherepanov, O. Bogershausen, A. Mulikdjanian, W. Junge, *Biochemistry* **1998**, *37*, 1131. doi:10.1021/BI9719152

- (b) A.-M. A. Hays, I. R. Vassiliev, J. H. Golbeck, R. J. Debus, *Biochemistry* **1999**, *38*, 11851. doi:10.1021/BI990716A
- (c) F. Rappaport, J. Lavergne, *Biochim. Biophys. Acta* **2001**, *1503*, 246. doi:10.1016/S0005-2728(00)00228-0
- (d) S. Nakamura, R. Nagao, R. Takahashi, T. Noguchi, *Biochemistry* **2014**, *53*, 3131. doi:10.1021/BI500237Y
- [6] (a) C. Tommos, L. Davidsson, B. Svensson, C. Madsen, W. Vermaas, S. Styring, *Biochemistry* **1993**, *32*, 5436. doi:10.1021/BI00071A020
- (b) X. S. Tang, D. A. Chisholm, G. C. Dismukes, G. W. Brudvig, B. A. Diner, *Biochemistry* **1993**, *32*, 13742. doi:10.1021/BI00212A045
- [7] S. Nakamura, T. Noguchi, *Biochemistry* **2015**, *54*, 5045. doi:10.1021/ACS.BIOCHEM.5B00568
- [8] H. Ishikita, E. W. Knapp, *Biophys. J.* **2006**, *90*, 3886. doi:10.1529/BIOPHYSJ.105.076984
- [9] K. Saito, A. W. Rutherford, H. Ishikita, *Proc. Natl. Acad. Sci. USA* **2013**, *110*, 7690. doi:10.1073/PNAS.1300817110
- [10] (a) A. W. Rutherford, W. Nitschke, in *Origin and Evolution of Biological Energy Conversion* (Ed. H. Baltscheffsky) **1996**, pp. 143–176 (Wiley-VCH: New York, NY).
- (b) A. W. Rutherford, P. Faller, *Philos. Trans. R. Soc. Lond. B Biol. Sci.* **2003**, *358*, 245. doi:10.1098/RSTB.2002.1186
- [11] P. Manna, R. LoBrutto, C. Eijkelhoff, J. P. Dekker, W. Vermaas, *Eur. J. Biochem.* **1998**, *251*, 142. doi:10.1046/J.1432-1327.1998.2510142.X
- [12] A. A. Stuchebrukhov, *Phys. Rev. E: Stat., Nonlinear, Soft Matter Phys.* **2009**, *79*, 031927. doi:10.1103/PHYSREVE.79.031927
- [13] K. Saito, T. Ishida, M. Sugiura, K. Kawakami, Y. Umena, N. Kamiya, J.-R. Shen, H. Ishikita, *J. Am. Chem. Soc.* **2011**, *133*, 14379. doi:10.1021/JA203947K
- [14] (a) G. T. Babcock, B. A. Barry, R. J. Debus, C. W. Hoganson, M. Atamian, L. McIntosh, I. Sithole, C. F. Yocum, *Biochemistry* **1989**, *28*, 9557. doi:10.1021/BI00451A001
- (b) P. Faller, R. J. Debus, K. Brettel, M. Sugiura, A. W. Rutherford, A. Boussac, *Proc. Natl. Acad. Sci. USA* **2001**, *98*, 14368. doi:10.1073/PNAS.251382598
- (c) A. W. Rutherford, A. Boussac, P. Faller, *Biochim. Biophys. Acta* **2004**, *1655*, 222. doi:10.1016/J.BBABIO.2003.10.016
- (d) C. Berthomieu, R. Hienerwadel, *Biochim. Biophys. Acta* **2005**, *1707*, 51. doi:10.1016/J.BBABIO.2004.03.011
- [15] (a) S. V. Ruffle, D. Donnelly, T. L. Blundell, J. H. A. Nugent, *Photosynth. Res.* **1992**, *34*, 287. doi:10.1007/BF00033446
- (b) B. Svensson, C. Etchebest, P. Tuffery, P. van Kan, J. Smith, S. Styring, *Biochemistry* **1996**, *35*, 14486. doi:10.1021/BI960764K
- [16] C. A. Buser, L. K. Thompson, B. A. Diner, G. W. Brudvig, *Biochemistry* **1990**, *29*, 8977. doi:10.1021/BI00490A014
- [17] (a) W. F. J. Vermaas, G. Renger, G. Dohnt, *Biochim. Biophys. Acta* **1984**, *764*, 194. doi:10.1016/0005-2728(84)90028-8
- (b) S. Styring, A. W. Rutherford, *Biochemistry* **1987**, *26*, 2401. doi:10.1021/BI00383A001
- [18] I. Vass, S. Styring, *Biochemistry* **1991**, *30*, 830. doi:10.1021/BI00217A037
- [19] J. Messinger, G. Renger, *Biochemistry* **1993**, *32*, 9379. doi:10.1021/BI00087A017
- [20] B. R. Brooks, R. E. Bruccoleri, B. D. Olafson, D. J. States, S. Swaminathan, M. Karplus, *J. Comput. Chem.* **1983**, *4*, 187. doi:10.1002/JCC.540040211
- [21] A. D. MacKerell Jr, D. Bashford, M. Bellott, R. L. Dunbrack Jr, J. D. Evanseck, M. J. Field, S. Fischer, J. Gao, H. Guo, S. Ha, D. Joseph-McCarthy, L. Kuchnir, K. Kuczera, F. T. K. Lau, C. Mattos, S. Michnick, T. Ngo, D. T. Nguyen, B. Prodhom, W. E. Reiher, B. Roux, M. Schlenkrich, J. C. Smith, R. Stote, J. Straub, M. Watanabe, J. Wiórkiewicz-Kuczera, D. Yin, M. Karplus, *J. Phys. Chem. B* **1998**, *102*, 3586. doi:10.1021/JP973084F
- [22] *QSite, version 5.8* **2012** (Schrödinger, LLC: New York, NY).
- [23] M. Petrek, M. Otyepka, P. Banas, P. Kosinova, J. Koca, J. Damborsky, *BMC Bioinformatics* **2006**, *7*, 316. doi:10.1186/1471-2105-7-316